C_2H_5OH containing 3 mL of 5 N KOH was heated on the steam bath for 30 min. The solvent was evaporated, and the residue was dissolved in H_2O. The solution was clarified by filtration and then neutralized. The base, **11**, that separated was left overnight and then filtered, and the filtrate was dried: yield 0.63 g (90%).

1-[[2-(Dimethylamino)ethyl]amino]-7-hydroxy-4-(hydroxymethyl)-9*H*-xanthen-9-one (12). Two grams (4.0 mmol) of the 9*H*-xanthen-9-one **39** gave, after treatment by the method used for **11**, 1.2 g (88%) of the desired phenolic product **12**, mp 199 °C dec after crystallization from CH_3OH.

2-(5-Chloro-2-methylphenoxy)-5-methoxybenzoic Acid (41). A mixture of 45 g (0.267 mol) of 5-methoxysalicyclic acid, 67.6 g (0.268 mol) of 4-chloro-2-iodotoluene, 50.3 g of dry K_2CO_3, and 3.0 g of Cu-bronze in 100 mL DMF was heated under reflux for 3 days. The cooled mixture was poured into a large volume of H_2O and extracted with ether. The layers were separated, and the aqueous phase was carefully acidified to furnish 51.1 g of the acid (65.4%), mp 185–187 °C after crystallization from acetic acid. Anal. ($C_{15}H_{13}ClO_4$) C, H.

1-Chloro-7-methoxy-4-methyl-9*H*-xanthen-9-one (42). A solution of 47.9 g (0.164 mol) of crude **41** in 240 mL of H_2SO_4 was heated on the steam bath for 1.5 h. The cooled solution was poured into ice–water and filtered, and the filter cake was washed with H_2O. The cyclization product was stirred with hot 8% NaOH solution, cooled, and filtered. The filter cake was washed with H_2O and dried: yield 20.3 g (45%). After two crystallizations from Me_2SO, the 9*H*-xanthen-9-one melted at 179–179.5 °C. Anal. ($C_{14}H_{11}ClO_4$) C, H.

1-[[2-(Diethylamino)ethyl]amino]-7-hydroxy-4-methyl-9*H*-xanthen-9-one (9). A solution of 3.72 g (13.5 mmol) of the chloro-9*H*-xanthen-9-one **42** and 25 mL of *N,N*-diethylethylenediamine was refluxed overnight in a flask protected from moisture. The cooled reaction mixture was diluted with H_2O and made strongly alkaline with KOH solution. The apparatus was set for downward distillation. A total of 100 mL of the solvent was distilled off, and the cooled reaction mixture was extracted with ether, which was concentrated to leave 4.55 g (95%) of crude **43**, mp 85.5–86.5 °C after crystallization from CH_3OH. Anal. ($C_{21}H_{26}N_2O_3$) C, H, N.

A solution of 1.38 g (3.9 mmol) of crude **43** in 15 mL of 56% HI solution was heated under reflux for 2.5 h. The cooled solution was filtered, and the solid was washed with ether. Upon recrystallization from CH_3OH–ether, there was obtained 0.8 g (44%) of the HI salt, mp 240–242 °C dec.

1-[[2-(Dimethylamino)ethyl]amino]-7-hydroxy-4-methyl-9*H*-xanthen-9-one (10). A solution of 4.38 g (15.9 mmol) of crude **42** in 30 mL of *N,N*-dimethylethylenediamine was refluxed overnight. After the usual workup as described in the preceding section, there was obtained 3.80 g (73%) of crude **43**. A solution of 1.30 g (4.0 mmol) of this compound in 15 mL of 56% HI was refluxed for 3.5 h. The mixture was left overnight, and the salt was collected on a filter, washed with ether, and dried. After crystallization from CH_3OH, there was obtained 0.70 g (40%) of the pure HI salt.

Acknowledgment. We are indebted to the National Cancer Institute for a grant (CA-19674) that supported most of the work reported here and also for the results of the antitumor tests.

Registry No. **1**, 3105-97-3; **2**, 479-50-5; **5**, 86455-90-5; **6**, 86455-91-6; **7**, 86455-92-7; **9**, 86455-93-8; **9**·HI, 86455-94-9; **10**, 86455-95-0; **10**·HI, 86455-96-1; **11**, 86455-97-2; **12**, 86455-98-3; **13**, 16807-37-7; **14**, 108-37-2; **15**, 86455-99-4; **16**, 86456-00-0; **17**, 86456-01-1; **18**, 86456-02-2; **18** fumarate, 86456-03-3; **19**, 86456-04-4; **20**, 86456-05-5; **21**, 86456-06-6; **22**, 86456-07-7; **23**, 86456-08-8; **24**, 86456-09-9; **25**, 86456-10-2; **26**, 86456-11-3; **27**, 2612-02-4; **28**, 625-99-0; **29**, 86456-12-4; **30**, 86456-13-5; **31**, 86456-14-6; **32**, 86456-15-7; **33**, 86456-16-8; **34**, 86456-17-9; **35**, 86456-18-0; **36**, 86456-19-1; **37**, 86456-20-4; **38**, 86456-21-5; **39**, 86456-22-6; **40**, 33184-48-4; **41**, 86456-23-7; **42**, 86456-24-8; **43**, 86456-25-9; **44**, 86456-26-0; **45**, 38605-72-0; **46**, 6469-87-0; **47**, 19058-08-3; i, 86456-27-1; 5-methoxydithiosalicylic acid, 19532-69-5; *N,N*-diethylethylenediamine, 100-36-7; *N,N*-dimethylethylenediamine, 108-00-9; 1-[[2-(diethylamino)ethyl]amino]-7-hydroxy-9*H*-thioxanthen-9-one, 86456-28-2; 1-[[2-(diethylamino)ethyl]amino]-7-(toluenesulfonyloxy)-9*H*-thioxanthen-9-one, 86456-29-3; 1-[[2-(diethylamino)ethyl]amino]-7-(toluenesulfonyloxy)-9*H*-thioxanthen-9-one fumarate, 86456-30-6; 1-[[2-(dimethylamino)-ethyl]amino]-7-hydroxy-9*H*-thioxanthen-9-one, 86456-31-7; 1-[[2-(diemthylamino)ethyl]amino]-7-(toluenesulfonyloxy)-9*H*-thioxanthen-9-one, 86456-32-8; 1-[[2-(diethylamino)ethyl]-amino]-4-(hydroxymethyl)-7-(toluenesulfonyloxy)-9*H*-thioxanthen-9-one, 86456-33-9; 1-[[2-(dimethylamino)ethyl]-amino]-9-oxo-9*H*-thioxanthene-4-carboxyaldehyde, 86470-89-5.

Structural Studies of Metyrapone: A Potent Inhibitor of Cytochrome P-450

Miriam Rossi*

The Institute for Cancer Research, The Fox Chase Cancer Center, Philadelphia, Pennsylvania 19111. *Received June 7, 1982*

The crystal and molecular structure of metyrapone, a powerful inhibitor of certain cytochromes P-450, is described. Cytochrome P-450 enzymes are involved in metabolic processes, including those activating insecticides, drugs, and carcinogens. Metyrapone inhibits both the adrenal cytochrome P-450 catalyzing 11-β-hydroxylation in steroid biosynthesis and most microsomal cytochromes P-450 induced by phenobarbital pretreatment. Crystal data are as follows: a = 11.828 (1), b = 6.268 (6), c = 18.269 (3) Å, β = 115.27 (1)°, V = 1224.9 (3) Å^3, space group $P2_1/c$, d_{calcd} = 1.227 g cm^{-3}, Z = 4. No intermolecular interactions are apparent in the solid state other than van der Waals forces. The torsion angle about the C(7)–C(10) bond to which the two 3-pyridyl groups are attached is 59.4 (1)°. The three negatively charged heteroatoms form a triangle; the nitrogen atoms are anti to the exocyclic oxygen and are 4.347 (1) Å apart. The N5–O11 distance is 5.850 (1) Å; the N14–O11 intramolecular distance is 4.750 (1) Å. The "twisted butterfly" conformation found for metyrapone is found in other molecules that are substrates and inducers of the specific cytochrome P-450 inhibited by metyrapone. The availability of nucleophilic functional groups is a feature common to most directly acting inhibitors of cytochrome P-450 enzymes and is manifested in metyrapone by the presence of the basic nitrogens. These factors may be necessary for interaction with the protein.

The literature on metyrapone suggests a bifunctional role for this clinically active drug.[1,2] It is an inhibitor of two classes of cytochrome P-450 enzymes: adrenal steroid 11-β-hydroxylase and most phenobarbital-inducible forms of cytochrome P-450 (P-450$_{PB}$) found in various tissues. Cytochromes P-450 are a group of inducible enzymes responsible for the oxidation of lipophilic compounds including drugs, steroids, and polycyclic aromatic hydrocarbons.[3] The different cytochrome P-450 enzymes cat-

* Corresponding Address: Department of Chemistry, Vassar College, Poughkeepsie, NY 12601.

(1) Liddle, G. W.; Island, D.; Lance, E. M.; Harris, A. P. *J. Clin. Endocrinol. Metab.* **1958**, *18*, 906.
(2) Leibman, K. C. *Mol. Pharmacol.* **1969**, *5*, 1.
(3) Lu, A. Y. H.; West, S. B. *Pharmaco. Rev.* **1980**, *31*, 277.

0022-2623/83/1826-1246$01.50/0

Table I. Refined Atomic Parameters of Metyrapone[a]

atom	x	y	z	B_{11}	B_{22}	B_{33}	B_{12}	B_{13}	B_{23}
O(11)	0.6434 (1)	−0.0545 (1)	0.6006 (1)	11.19 (4)	2.68 (3)	6.33 (4)	−1.17 (3)	5.53 (5)	−0.65 (3)
N(5)	0.8352 (1)	0.7072 (2)	0.8007 (1)	5.38 (4)	3.59 (4)	4.89 (4)	−0.74 (3)	1.57 (4)	−0.66 (4)
N(14)	0.8081 (1)	0.5333 (2)	0.5133 (1)	5.23 (3)	4.36 (4)	4.38 (3)	−0.40 (3)	2.63 (4)	0.28 (4)
C(1)	0.7438 (1)	0.3862 (2)	0.7256 (1)	3.55 (3)	2.73 (3)	2.82 (3)	0.19 (3)	1.59 (3)	0.30 (3)
C(2)	0.8566 (1)	0.2810 (2)	0.7668 (1)	3.99 (3)	3.52 (4)	4.09 (4)	0.63 (3)	1.77 (4)	0.07 (4)
C(3)	0.9572 (1)	0.3911 (3)	0.8235 (1)	3.54 (4)	5.92 (7)	4.85 (5)	0.56 (4)	1.19 (4)	0.21 (5)
C(4)	0.9422 (1)	0.6019 (2)	0.8378 (1)	4.36 (4)	5.28 (6)	4.72 (5)	−1.14 (5)	1.34 (5)	−0.72 (5)
C(6)	0.7394 (1)	0.5980 (2)	0.7460 (1)	4.24 (4)	2.89 (4)	3.84 (4)	0.15 (3)	1.38 (4)	−0.10 (3)
C(7)	0.6291 (1)	0.2703 (2)	0.6642 (1)	3.53 (3)	2.61 (4)	3.26 (3)	0.00 (3)	1.51 (3)	0.14 (3)
C(8)	0.5224 (1)	0.4202 (2)	0.6109 (1)	3.65 (4)	4.13 (5)	4.29 (5)	0.48 (4)	1.10 (4)	0.28 (4)
C(9)	0.5801 (1)	0.1234 (2)	0.7118 (1)	5.07 (4)	3.74 (5)	4.80 (5)	−0.52 (4)	2.83 (5)	0.18 (4)
C(10)	0.6642 (1)	0.1355 (2)	0.6068 (1)	4.60 (4)	2.67 (4)	3.21 (4)	−0.11 (3)	1.52 (4)	−0.03 (3)
C(12)	0.7197 (1)	0.2356 (2)	0.5549 (1)	3.43 (3)	3.11 (4)	2.84 (3)	0.16 (3)	1.10 (3)	−0.06 (3)
C(13)	0.7584 (1)	0.4469 (2)	0.5600 (1)	4.50 (3)	3.23 (4)	3.54 (4)	0.07 (3)	2.03 (4)	0.11 (3)
C(15)	0.8192 (1)	0.4064 (3)	0.4583 (1)	5.57 (4)	6.02 (7)	4.29 (4)	−0.41 (4)	2.92 (5)	0.00 (5)
C(16)	0.7841 (1)	0.1956 (2)	0.4485 (1)	6.81 (5)	5.86 (7)	4.52 (5)	−0.62 (5)	3.46 (6)	−1.28 (5)
C(17)	0.7343 (1)	0.1085 (2)	0.4971 (1)	5.16 (4)	3.98 (5)	3.86 (4)	−0.32 (4)	2.02 (4)	−0.83 (4)
H(2)	0.864 (1)	0.134 (2)	0.757 (1)	4.9 (3)					
H(3)	1.034 (1)	0.324 (2)	0.851 (1)	7.4 (4)					
H(4)	1.014 (1)	0.685 (2)	0.879 (1)	6.4 (4)					
H(6)	0.662 (1)	0.680 (2)	0.719 (1)	4.9 (3)					
H(13)	0.751 (1)	0.542 (2)	0.600 (1)	4.6 (3)					
H(15)	0.854 (1)	0.473 (2)	0.422 (1)	6.0 (4)					
H(16)	0.791 (1)	0.114 (3)	0.409 (1)	7.6 (4)					
H(17)	0.712 (1)	−0.046 (2)	0.494 (1)	5.7 (3)					
H(80)	0.457 (1)	0.341 (3)	0.568 (1)	7.3 (4)					
H(81)	0.482 (1)	0.485 (2)	0.644 (1)	5.6 (3)					
H(82)	0.548 (1)	0.539 (2)	0.584 (1)	5.5 (3)					
H(90)	0.647 (1)	0.021 (2)	0.749 (1)	5.0 (3)					
H(91)	0.503 (1)	0.044 (3)	0.672 (1)	8.0 (4)					
H(92)	0.550 (1)	0.214 (2)	0.745 (1)	6.0 (4)					

[a] Positional parameters are listed as fractions of cell edges. Anisotropic temperature factors are expressed as $\exp[-1/4(h^2a^{*2}B_{11} + k^2b^{*2}B_{22} + l^2c^{*2}B_{33} + 2hka^*b^*B_{12} + 2hla^*c^*B_{13} + 2klb^*c^*B_{23})]$ and isotropic temperature factors are listed as $\exp(-B \sin^2 \theta/\lambda^2)$ with B values given in Å^2. Estimated standard deviations with respect to the last digit listed are given in parentheses.

alyze at least ten distinct chemical oxidation reactions, including aliphatic and aromatic hydroxylation, N-oxidation, and epoxidation. In these reactions, detoxification of many compounds occurs in the liver, but some of the reactive epoxide intermediate species are carcinogenic. In the adrenal cortex, the cytochrome P-450 enzymes contribute to steroid synthesis by catalyzing oxidative degradation of cholesterol. Metyrapone is used as a diagnostic and therapeutic tool because it inhibits the 11-β-hydroxylation of deoxycorticosterone to corticosterone and deoxycortisol to cortisol. Synthesis of aldosterone and cortisol, then, is prevented.

In eukaryotes, it is known that an extremely wide range of drugs, carcinogens, insecticides, and other foreign compounds induce cytochrome P-450 activity. As recently reviewed by Testa and Jenner,[4] inhibition of cytochrome P-450 mediated reactions also occurs by many different mechanisms. This is principally due to the different isozymes of cytochrome P-450 that exist. However, differences in levels of induction and inhibition are evident between species[5] and within the same species as a function of sex and age.[6] The mechanism of the induction process in rat hepatic cells by both phenobarbital (PB)[7] and 3-methylcholanthrene (3MC)[8] proceeds with an evident increase in the cytoplasmic mRNA concentration. Many forms of cytochrome P-450 are then produced, but one type ($P\text{-}450_{PB}$ or $P\text{-}450_{PAH}$, respectively) predominates. These proteins catalyze position-specific hydroxylations. Metyrapone is a stronger ligand for PB-induced forms of cytochrome P-450.

The complicated nature of this enzyme system has made the understanding of the mechanistic details difficult. Reported in the literature are such apparent anomalies as inhibitors that are substrates (e.g., metyrapone), inducers that are weak inhibitors (e.g., 5,6-benzoflavone), and inducers that are substrates (e.g., PB and 3MC). It has even been shown that the same molecule that inhibits one type of cytochrome P-450 is an activator of another cytochrome P-450 enzyme.[9] By studying the molecular structures of different molecules that interact with the cytochrome P-450 enzyme system, we hope to obtain clues about the specificity. We have already reported the structures of two isomeric molecules that perform different functions toward cytochrome P-450. One is 7,8-benzoflavone, an inhibitor of the cytochrome P-450 responsible for the metabolism of polycyclic aromatic hydrocarbons ($P\text{-}450_{PAH}$). The other is 5,6-benzoflavone, a structural isomer that is an inducer (and weak inhibitor) of cytochrome $P\text{-}450_{PAH}$.[10] The crystal and molecular structure of metyrapone, a potent inhibitor of PB-inducible forms of cytochrome P-450, are now presented. Structural differences and similarities between molecules that are inhibitors, inducers, and substrates of this enzyme system are discussed.

Results and Discussion

Description of the Structure. The structural pa-

(4) Testa, B.; Jenner, P. *Drug Metab. Rev.* **1981**, *12*, 1.
(5) Kremers, P.; Beaune, P.; Cresteil, T.; DeGraeve, J.; Columelli, S.; Leroux, J.; Gielen, J. E. *Eur. J. Biochem.* **1981**, *118*, 599.
(6) Kao, J.; Hudson, P. *Biochem. Pharmacol.* **1980**, *29*, 1191.
(7) Adesnok, M.; Bar-Nun, S.; Maschio, F.; Zurich, M.; Lippman, A.; Bard, E. *J. Biol. Chem.* **1981**, *256*, 10340.
(8) Loeb, L. A.; Gelboin, H. V. *Proc. Natl. Acad. Sci. U.S.A.* **1964**, *52*, 1219.
(9) Thorgeirsson, S. S.; Atlas, S. A.; Boobis, A. R.; Felton, J. S. *Biochem. Pharmacol.* **1979**, *28*, 217.
(10) Rossi, M.; Cantrell, J. S.; Farber, A. J.; Dyott, T.; Carrell, H. L.; Glusker, J. P. *Cancer Res.* **1980**, *40*, 2774.

Table II. Bond Lengths, Bond Angles, and Torsion Angles

A. Bond Lengths and Their Standard Deviations

	length, Å		length, Å
C(1)-C(2)	1.387 (1)	C(15)-C(16)	1.374 (2)
C(1)-C(6)	1.386 (1)	C(16)-C(17)	1.371 (2)
C(1)-C(7)	1.525 (1)	C(2)-H(2)	0.95 (1)
C(2)-C(3)	1.383 (2)	C(3)-H(3)	0.93 (1)
C(3)-C(4)	1.372 (2)	C(4)-H(4)	1.01 (1)
C(4)-N(5)	1.327 (1)	C(6)-H(6)	0.98 (1)
N(5)-C(6)	1.336 (1)	C(8)-H(80)	0.97 (1)
C(7)-C(8)	1.541 (1)	C(8)-H(81)	1.00 (1)
C(7)-C(9)	1.539 (1)	C(8)-H(82)	1.00 (1)
C(7)-C(10)	1.535 (1)	C(9)-H(90)	1.02 (1)
C(10)-O(11)	1.211 (1)	C(9)-H(91)	1.02 (1)
C(10)-C(12)	1.502 (1)	C(9)-H(92)	1.00 (1)
C(12)-C(13)	1.391 (2)	C(13)-H(13)	0.97 (1)
C(12)-C(17)	1.391 (2)	C(15)-H(15)	1.00 (1)
C(13)-N(14)	1.341 (1)	C(16)-H(16)	0.92 (1)
N(14)-C(15)	1.330 (2)	C(17)-H(17)	1.00 (1)

B. Bond Angles and Their Standard Deviations

	angle, deg		angle, deg
C(2)-C(1)-C(6)	116.5 (1)	C(1)-C(2)-H(2)	120.3 (6)
C(2)-C(1)-C(7)	121.4 (1)	C(3)-C(2)-H(2)	120.4 (6)
C(6)-C(1)-C(7)	122.0 (1)	C(2)-C(3)-H(3)	120.6 (1.0)
C(1)-C(2)-C(3)	119.3 (1)	C(4)-C(3)-H(3)	120.5 (1.0)
C(2)-C(3)-C(4)	118.9 (1)	C(3)-C(4)-H(4)	120.3 (8)
C(3)-C(4)-N(5)	123.6 (1)	N(5)-C(4)-H(4)	116.1 (7)
C(4)-N(5)-C(6)	116.5 (1)	N(5)-C(6)-H(6)	114.8 (8)
N(5)-C(6)-C(1)	125.1 (1)	C(1)-C(6)-H(6)	120.1 (8)
C(1)-C(7)-C(8)	113.9 (1)	C(7)-C(8)-H(80)	110.9 (9)
C(1)-C(7)-C(9)	107.5 (1)	C(7)-C(8)-H(81)	109.5 (8)
C(1)-C(7)-C(10)	110.4 (1)	C(7)-C(8)-H(82)	115.2 (6)
C(8)-C(7)-C(9)	108.5 (1)	H(80)-C(8)-H(81)	105.8 (9)
C(8)-C(7)-C(10)	106.9 (1)	H(80)-C(8)-H(82)	106.7 (1.2)
C(9)-C(7)-C(10)	109.5 (1)	H(81)-C(8)-H(82)	108.2 (1.0)
O(11)-C(10)-C(7)	120.1 (1)	C(7)-C(9)-H(90)	112.5 (5)
O(11)-C(10)-C(12)	118.5 (1)	C(7)-C(9)-H(91)	109.0 (9)
C(7)-C(10)-C(12)	121.3 (1)	H(90)-C(9)-H(91)	112.1 (1.2)
C(10)-C(12)-C(13)	125.1 (1)	H(90)-C(9)-H(92)	108.6 (1.1)
C(10)-C(12)-C(17)	118.0 (1)	H(91)-C(9)-H(92)	105.6 (1.0)
C(13)-C(12)-C(17)	116.9 (1)	C(12)-C(13)-H(13)	120.2 (6)
N(14)-C(13)-C(12)	124.3 (1)	N(14)-C(13)-H(13)	115.5 (6)
C(13)-N(14)-C(15)	116.8 (1)	N(14)-C(15)-H(15)	116.4 (8)
N(14)-C(15)-C(16)	123.5 (1)	C(16)-C(15)-H(15)	120.1 (8)
C(15)-C(16)-C(17)	119.2 (1)	C(15)-C(16)-H(16)	120.7 (9)
C(16)-C(17)-C(12)	119.3 (1)	C(17)-C(16)-H(16)	120.1 (9)
C(7)-C(9)-H(92)	108.7 (8)	C(12)-C(17)-H(17)	118.5 (7)
		C(16)-C(17)-H(17)	122.2 (7)

C. Torsion Angles

	angle, deg		angle, deg
C(1)-C(7)-C(10)-C(12)	−59.4 (1)	C(2)-C(1)-C(7)-C(9)	72.8 (1)
C(17)-C(12)-C(10)-O(11)	5.5 (2)	C(6)-C(1)-C(7)-C(8)	16.3 (2)
C(13)-C(12)-C(10)-O(11)	−174.2 (1)	C(6)-C(1)-C(7)-C(9)	−104.0 (1)
C(2)-C(1)-C(7)-C(8)	−166.9 (1)		

rameters and conformation of metyrapone are presented in Figure 1 and Table I. Intramolecular bond distances, bond angles, and torsion angles are listed in Table II. The molecular structure of metyrapone is characterized by a twist of the molecule about the central two-carbon link (C7–C10) connecting the two pyridine rings. The torsion angle C1–C7–C10–C12 is 59.4 (1)°. The observed conformation is such that the two nitrogen atoms, N5 and N14, are on the same side of the molecule but opposite the carbonyl oxygen 011 (i.e., N5 and N14 are anti to 011), as shown in Figure 1. The heteroatoms form a triangle with intramolecular distances as follows: N5–N14, 4.347 (1) Å; N5–011, 5.850 (1) Å; N14–011, 4.750 (1) Å (Figure 2). Examination of the unit cell packing (Figure 3) reveals no strong intermolecular interactions (e.g., hydrogen bonding, stacking) other than those due to van der Waals forces. The electronic structure of metyrapone is such that only hydrogen-bond acceptors are present (i.e., the pyridyl nitrogens and carbonyl oxygen); therefore, hydrogen bonding is not possible. The short intermolecular contacts evident in the crystal structure involve the negatively charged heteroatoms and protons and are given in Table III. These primarily hydrophobic interactions may be of importance in determining the mechanism by which metyrapone inhibits the cytochrome P-450 enzymes.

The structural parameters agree with standard values for compounds containing similar functional groups, e.g., nicotinic acid[11] and nicotinamide.[12] The pyridyl groups in all these independent determinations were approxi-

(11) (a) Gupta, M. P.; Kumar, P. *Cryst. Struct. Commun.* **1975**, *4*, 365. (b) Wright, W. B.; King, G. S. D. *Acta Crystallogr.* **1953**, *6*, 305.

(12) Wright, W. B.; King, G. S. D. *Acta Crystallogr.* **1954**, *7*, 283.

Table III. Short Intermolecular Contacts in Metyrapone

D-H···A	acceptor position	D-H, Å	D···A, Å	H···A, Å	D-H···A, deg
C6-H6···O11	$x, y-1, z$	0.98 (1)	3.243 (1)	2.66 (1)	118.1 (8)
C8-H82···O11	$x, y-1, z$	1.00 (1)	3.627 (1)	2.75 (1)	145.8 (8)
C13-H13···O11	$x, y-1, z$	0.97 (1)	3.610 (2)	2.84 (1)	137.3 (6)
C2-H2···N5	$x, y+1, z$	0.95 (1)	3.677 (1)	2.85 (1)	145.2 (6)
C15-H15···N5	$x, {}^3/_2+y, {}^1/_2+z$	1.00 (1)	3.829 (2)	2.93 (1)	150.0 (8)
C16-H16···N5	$x, {}^1/_2-y, {}^1/_2+z$	0.92 (1)	3.928 (2)	3.02 (1)	170.2 (9)
C9-H90···N5	$x, y+1, z$	1.02 (1)	3.791 (1)	2.82 (1)	159.7 (5)
C3-H3···N14	$2-x, -{}^1/_2+y, {}^1/_2-z$	0.93 (1)	3.816 (1)	3.00 (1)	147.3 (1.0)
C4-H4···N14	$2-x, -{}^3/_2+y, {}^1/_2-z$	1.01 (1)	4.071 (1)	3.09 (1)	166.0 (7)
C17-H17···N14	$x, y+1, z$	1.00 (1)	3.692 (1)	2.83 (1)	144.4 (7)
C8-H80···N14	$1-x, 1-y, 1-z$	0.97 (1)	3.598 (1)	2.94 (1)	125.7 (9)

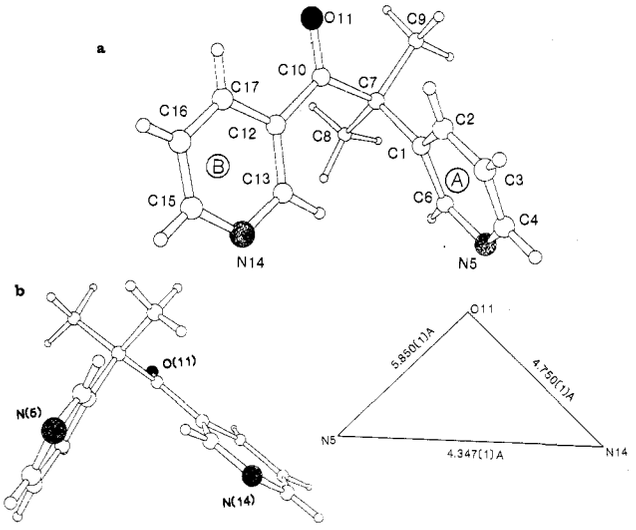

Figure 1. Two views of metyrapone, illustrating the three-dimensional character of the molecule: (a) the numbering and labeling scheme for metyrapone; (b) the gauche orientation of the pyridyl nitrogens to each other and to the carbonyl oxygen.

mately planar. In metyrapone, the average deviation from planarity for both 3-pyridyl groups is 0.005 (1) and 0.003 (1) Å, respectively. The torsion angle about the C12–C10 bond is approximately 5.5°, placing O11 0.101 (1) Å away from the plane of the 3-pyridyl group (containing N14) adjacent to it. Crystal structures, such as nicotinic acid and nicotinamide, described above, have apparent greater intermolecular interactions and show greater displacements of the oxygen, varying from 0.30 to 0.46 Å.

Inhibition of the Enzyme. Inhibition of the cytochrome P-450 enzymes by a particular inhibitor molecule involves structural and electronic recognition between the inhibitor and the protein. In metyrapone, this recognition occurs with both oxidized [Fe(II)] and reduced [Fe(III)] forms of cytochromes P-450. Therefore, the literature describing metyrapone inhibition reactions is intricate. The absorption spectrum of the metyrapone–cytochrome P-450 complex shows a shift to lower wavelengths by the heme Soret band (type II binding), as do other pyridine derivative inhibitors. From this, it was deduced that metyrapone binds directly to the heme iron.[13] It was shown in the bacterial *Pseudomonas putida* cytochrome P-450 that metyrapone inhibition of camphor hydroxylation was competitive with substrate binding.[13] The active site (where the substrate binds) was described as being close to the "oxygen-activating" site. Early attempts to determine the mechanism by which metyrapone inhibits the metabolism in rat liver cells of various substrates (e.g., hexobarbital, trichloroethylene, morphine)[14] established that in certain cases the presence of substrate did not affect the degree of inhibition; i.e., the inhibition is noncompetitive. Oxygen binding, not substrate binding, was believed to be impaired in those cases. Other kinetic inhibition studies in rat liver cells showed metyrapone to be noncompetitive at low concentrations but competitive at high concentrations.[15] These results are consistent with the interpretation that metyrapone can interfere with both substrate binding to the oxidized cytochrome P-450 and oxygen binding to the reduced form of cytochrome P-450. Metabolites of metyrapone are mainly N-oxidized at the two pyridyl groups;[16] these metabolites are more polar than the parent compound and may themselves be involved in inhibition.

Structure–activity studies were carried out on metyrapone to determine the active part of the molecule in inhibition of steroid 11-β-hydroxylase. Compounds were synthesized that had 65% the potency inhibited by metyrapone.[17] Activity required pyridine A (the 3-pyridyl group α to the methyl-substituted carbon atom) and the steric bulk provided by an aromatic group (e.g., pyridyl, phenyl) at position B (Figure 1). Reduction of the carbonyl group to the alcohol proved to be an acceptable change, indicating variation in the oxidation state of the oxygen is possible. Phenyl substitution of either methyl group also led to retention of activity. Thus, essential parts of the structure required for activity are organized around a tetrahedral carbon atom. This configuration confers limited rotational flexibility about this carbon center. This essential "core" as found from these structure–activity studies on metyrapone is illustrated in Figure 3. It is this "core" that, because of steric interaction between ring A and the methyl groups, causes the molecular structure of metyrapone to be twisted. Some cytochrome P-450 substrates (phenobarbital, DDT) and inhibitors (SKF-525A, SKF-12185, amphenone B) also have similar steric interactions because of their functional groups. These interactions result (or are expected to) in the "twisted butterfly" solid-state conformation. It appears that interactions with the cytochrome P-450$_{PB}$ active site can accommodate this spatial requirement. This contrasts with the more planar structural conformation required for molecular interactions at the cytochrome P-450$_{PAH}$ active site. Experimental evidence for this observation was obtained from studies done on dichlorinated biphenyls.[18] The pattern of chlorine

(13) Peterson, J. A.; Ullrich, V.; Hildebrandt, A. G. *Arch Biochem. Biophys.* **1971**, *145*, 531.
(14) Leibman, K. C.; Hildebrandt, A. G.; Estabrook, R. W. *Biochem. Biophys. Res. Commun.* **1969**, *36*, 789.
(15) Hildebrandt, A. G. "Biological Hydroxylation Mechanisms"; Boyd, G. S.; Smellie, R. M. S., Eds.; Academic Press: New York, 1972; p 79.
(16) Damani, L. A.; Crooks, P. A.; Gorrod, J. W. *J. Pharm. Pharmacol.* **1979**, *31*, 94P.
(17) Napoli, J. L.; Counsell, R. E. *J. Med. Chem.* **1977**, *20*, 762.

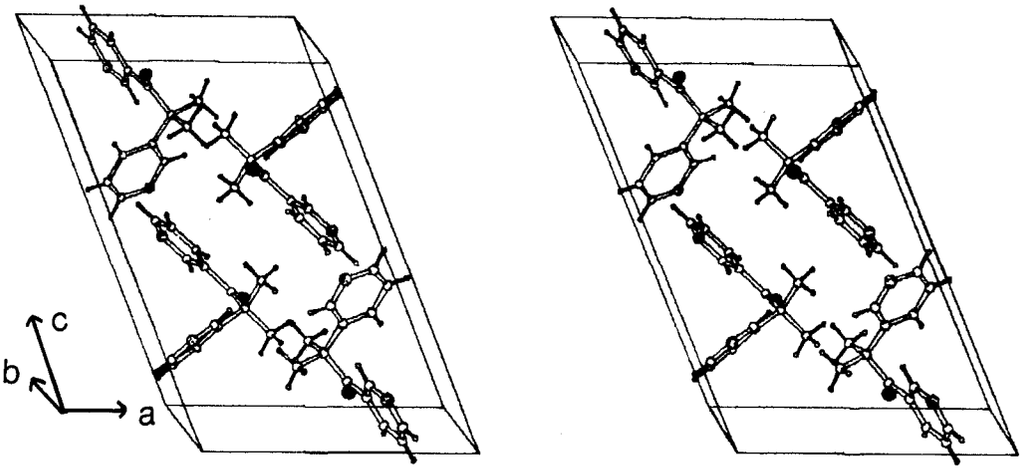

Figure 2. View of the unit cell contents and crystal packing of metyrapone. There is no hydrogen bonding, nor stacking interactions; only van der Waals forces are present in the crystal structure.

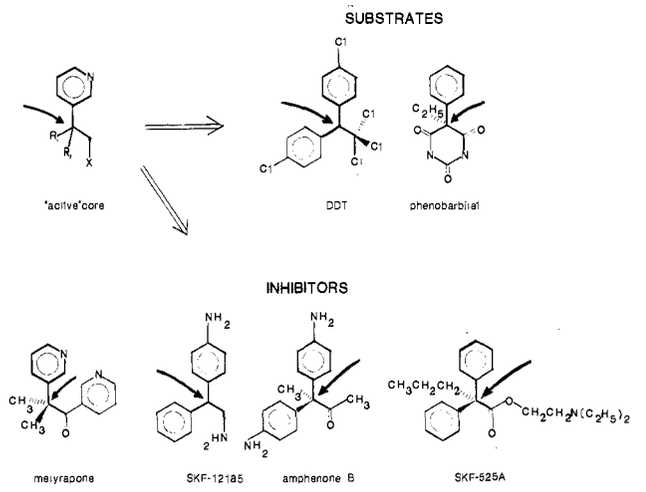

Figure 3. The pharmaceutically active "core" of metyrapone, as determined from structure–activity studies,[17] is shown, along with known inhibitors and substrates of cytochrome P-450$_{PB}$. Structures with an asterisk have been studied crystallographically: (a) "active core" of metyrapone; (b) DDT*; (c) phenobarbital*; (d) SKF-525A; (e) metyrapone*; (f) SKF-12185; (g) amphenone B.

substitution on biphenyl had a distinct effect on whether cytochrome P-450$_{PB}$ or P-450$_{PAH}$ was used in its metabolism. Halogen substitutions at sites that resulted in more planar biphenyl structures were metabolized via cytochrome P-450$_{PAH}$; more twisted biphenyl derivatives were metabolized by cytochrome P-450$_{PB}$.

Drug Recognition. Necessary requirements for both drug recognition and enzyme–substrate interactions are steric fit to the receptor, appropriately distributed charge density, and sufficient lipophilicity to allow easy access into membranes. By using techniques to determine and quantify factors involved in drug–receptor interactions, the surface structural features of some drugs that interact in a functionally different manner with the PB-inducible forms of cytochrome P-450 were compared. It should be noted that although most substrates, such as DDT and PB, can induce cytochrome P-450 activity, the site of this induction is a separate structural problem not addressed in this study. The molecular volume is a three-dimensional description of the volume occupied by a molecule in which each of the constituent atoms is represented by a sphere

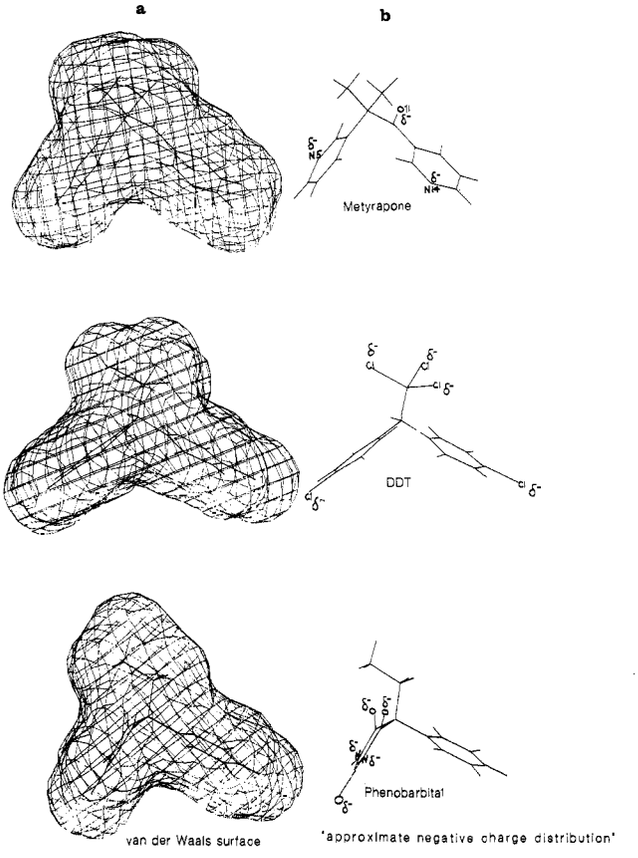

Figure 4. (a) Comparison of molecular volumes as calculated from van der Waals radii for: (1) metyrapone (inhibitor), (2) DDT (inducer/substrate), and (3) phenobarbital (inducer/substrate). Note the pseudo-three-fold symmetry about the tetrahedral carbon atoms. (b) Estimated negative charge distribution of these same molecules.

with a radius derived from its van der Waals radius. This provides a view of the overall shape of the molecule. The van der Waals surfaces for metyrapone, phenobarbital,[19] and DDT[20] have been calculated based on the crystallographic coordinates of each molecule by using Monte Carlo techniques[21] and are illustrated in Figure 4. The resulting

(18) Kaminsky, L. S.; Kennedy, M. W.; Adams, S. M.; Guengerich, F. P. *Biochemistry* **1981**, *20*, 7379.
(19) Williams, P. P. *Acta Crystallogr., Sect. B* **1973**, *B29*, 1572.
(20) Delacy, T. P.; Kennard, C. H. *J. Chem. Soc., Perkin Trans. 2* **1972**, 2148.
(21) Kumosinski, T. F.; Amato, S. V.; Liebman, M. N. *Biophys. J.* **1982**, *37*, 398A W-AM-P0127.

surfaces are similar, and all three molecules have a common region consisting of a tetrahedral core in the restricted "twisted butterfly" conformation. Additionally, the molecular shapes may be described as having pseudo-threefold symmetry about the tetrahedral carbon center. This spatial arrangement, as discussed under Inhibition of the Enzyme, permits accomodation of the bulky groups, such as phenyl, substituted phenyl, and pyridyl groups, found in these drugs. These aromatic, hydrophobic groups may be needed for binding to lipophilic regions of the enzyme. The fact that the three molecules are topologically similar while being functionally different in activity toward cytochrome P-450$_{PB}$ is suggestive that other physiochemical parameters are of importance.

A more complete description of molecular properties can be obtained by combining information about charge density with molecular surface. Examination of the electrostatic potential surface provides a way to evaluate the potential field about a molecule. It has been demonstrated that ab initio techniques are more accurate[22] compared to semiempirical approximations in calculating the net atomic charges needed for the electrostatic potential. Nonetheless, we have used approximate molecular orbital techniques in this first stage of analysis to estimate net atomic charges for these molecules.[23] The results obtained, in all cases, are consistent with chemical intuition regarding electronegativity. That is, in metyrapone, excess negative charge resides on the carbonyl oxygen and pyridyl nitrogens. For DDT, the negative charge was greatest about the two para-substituted chlorine atoms, followed by the centrally substituted chlorines; in PB, the greatest negative charge was about the heteroatoms. Recently, Craven et al. have completed experimental charge density studies on barbital[24] (the parent compound of PB). Net charges obtained for these atoms are consistent with the theoretical approximate molecular orbital determinations done by Voet[25] and by us on the barbital system. These are schematically illustrated in Figure 4. Unfortunately, it is difficult to make general statements about the different functions displayed by the three molecules. Based on topological arguments, because of the pseudo-three-fold symmetry exhibited by all of them, it appears that perhaps these "lobes" are necessary for a fit into the active site. The charge density and hydrophobicity of these lobes might determine how the molecule complements the active site of the enzyme.

Summarizing these characteristics for the three molecules shows that metyrapone, the inhibitor, has negative charges at all three lobes, contains three heteroatoms (including two basic nitrogens), and exhibits no hydrogen bonding in the crystal structure. A common feature in almost all the inhibitors that are directly acting or metabolically activated as described by Testa and Jenner[4] is the availability of nucleophilic functional groups capable of binding to cytochrome P-450. Such binding can prevent either of two steps in the catalytic cycle: the reduction of the cytochrome P-450 and/or the binding of molecular oxygen. Hydrophobic and other interactions were also found to be important. Phenobarbital, a substrate, shows a concentration of negative charge at only one lobe, due to the heteroatoms present. The other two show no charge density. The crystal structures of phenobarbital and other barbiturates illustrate their capacity for extensive hydrogen bonding. DDT, another substrate, resembles metyrapone in two ways. There are negative charges present at all three lobes, and it has no strong intermolecular forces in the crystal structure. It appears to rely on hydrophobic interactions. Clearly, this analysis of three molecules is not enough to specify the exact pharmacophore(s) needed for the various functions toward the cytochrome P-450 enzymes. More compounds in this series need to be analyzed. The molecular structures of other inhibitors of the cytochrome P-450 enzymes are currently under investigation.

Experimental Section

Metyrapone (2-methyl-1,2-di-3-pyridyl-1-propanone; metopirone) was obtained from the Aldrich Chemical Co., Inc., and through the generosity of Charles A. Brownley, Jr., of CIBA Pharmaceutical Co. It was crystallized by slow evaporation of a 1:1 hexane/ether solution as colorless plates.

Initial photographic studies showed the $2/m$ Laue symmetry and systematic absences in $h0l$ with l = odd and in $0k0$ with k = odd, thus uniquely defining the space group as $P2_1/c$. Unit cell dimensions were obtained by a least-squares fit to the angular settings of 10 centered reflections on a Syntex $P2_1$ diffractometer equipped with a graphite monochromator crystal. Crystal data for metyrapone, $C_{14}H_{14}N_2O$, molecular weight 226.28: a = 11.828 (1) Å, b = 6.2681 (6), c = 18.269 (3), β = 115.27 (1)°, V = 1224.9 (3) Å^3, d_{calcd} = 1.227 g cm^{-3}, Z = 4, space group $P2_1/c$; μ (Cu $K\alpha$) = 5.49 cm^{-1}. The crystal chosen for intensity measurement was cut from a larger crystal into the following dimensions: (100 - $\bar{1}$00) 0.28 × (010 - 0$\bar{1}$0) 0.23 × (001 - 00$\bar{1}$) 0.25 mm, and mounted approximately along the a axis on a glass fiber. Intensity measurements were made with Cu $K\alpha$ (λ = 1.5418 Å) radiation utilizing the θ-2θ scan technique; individual scan speeds were determined by a rapid scan at the position of the calculated Bragg peak, and the rate of scanning varied from 2.0 deg min^{-1} (less than 50 counts during the rapid scan) to 29.3 deg min^{-1} (more than 500 counts during the rapid scan). Three reflections were routinely monitored at intervals of 100 reflections; some decay as a function of time seemed apparent, but the deviation of the standards from their mean intensity varied only from 3.5 to 5% during the data collection. A decay correction was applied to the data. All reflections in the hkl and $-hkl$ octants to 2θ = 134° (sin θ/λ = 0.597 Å^{-1}) were collected. In addition, at the end of the data collection, the initial set of reflections ($0kl$) were recollected to determine if there was any effect of decay on these intensity measurements. The total number of data collected was 2883; an agreement factor of 0.024 was obtained for reflections measured more than once. The unique set of data then numbered 2286, of which 1952 reflections had $I > 2.0\sigma(I)$; these formed the basis of the structural solution and refinement, where $\sigma(I)$ was derived from counting statistics. Values of $\sigma(F)$ were determined from the equation $\sigma(F) = (F/2)[[\sigma^2(I)]/I^2 + \delta^2]^{1/2}$, where δ is estimated as the instrumental uncertainty (δ = 0.020) obtained from the variation in measured intensities in the periodically scanned standard reflections. The 1952 reflections and their associated standard deviations were corrected for Lorentz and polarization effects; no absorption correction was applied.

The structural solution, the positions of the 17 heavy atoms, was obtained by using MULTAN;[26] 200 E's greater than 2.0 were used, and the solution with the lowest residual (19.42) and the highest absolute figure of merit (1.077) was chosen to produce an E map which revealed the salient features of the structure, the positions of the 17 heavy atoms. Four cycles of isotropic, followed by two of anisotropic, full-matrix least-squares refinements minimizing $\sum\omega||F_o| - |F_c||^2$ reduced the R value ($R = \sum||F_o| - |F_c||/|F_o|$) to 0.108. The weights of the reflections, ω, during the refinement were $1/\sigma^2(F)$ with zero weight for those reflections with intensities below the threshold value [$2.0 < \sigma(I)$]. All hydrogen atoms were then located from a difference map. The

(22) Preston, H. J. T.; Kerman, E.; Kaufman, J. J.; Cusachs, L. C. *Int. J. Quantum Chem.* **1978**, *13*, 457.
(23) Pople, J. A.; Beveridge, D. L. "Approximate Molecular Orbital Theory"; McGraw-Hill: New York, 1970; Appendix A.
(24) Craven, B. M.; Fox, R. O., Jr.; Weber, H. P. *Acta Crystallogr., Sect. B* **1982**, *B38*, 1942.
(25) Voet, D. *J. Am. Chem. Soc.* **1972**, *94*, 8213.
(26) Germain, G.; Main, P.; Woolfson, M. M. *Acta Crystallogr., Sect. A* **1971**, *A27*, 368.

structure was refined further with anisotropic heavy atoms (C, N, and O) and isotropic hydrogen atoms to convergence at R = 0.043. At this point, analysis of the agreement between calculated and observed structure factors suggested the presence of secondary extinction ($F_c > F_o$), which affected the strongest low-order reflections: the (20-4), (200), and (202) reflections (with $\sin\theta/\lambda \leq 0.131$ Å^{-1}). Correction for secondary extinction and a final cycle of refinement produced the residuals R = 0.036 and weighted R = 0.047 by using the 1952 observed reflections. The final difference map showed no significant peaks.

Computer programs used were from the CRYSNET package.[27] The full-matrix least-squares program was UCLALS4,[28] modified by H. L. Carrell.[29] Other programs for the structural solution and plotting (VIEW and DOCK) were developed at the Institute for Cancer Research.[30] The atomic scattering factors used for oxygen, nitrogen, and carbon atoms[31] and for hydrogen atoms are listed in the literature.[32] Final positional and thermal parameters are listed in Table I. Lists of calculated and observed structure factors are available (see paragraph at end of paper regarding supplementary material).

Acknowledgment. This research was supported by American Cancer Society Grants IN-140 and BC-242, by National Institutes of Health Grants CA-10925, CA-22780, CA-06927, and RR 05539, and by an appropriation from the Commonwealth of Pennsylvania. I would especially like to thank Dr. Jenny Glusker for her valuable suggestions, patience, and support throughout this work. The author also acknowledges enlightening conversations with Drs. Murray-Rust and Liebman and the members of the crystallographic laboratories at The Institute for Cancer Research. In addition, special thanks are extended to the editor and reviewers for helpful comments and suggestions.

Registry No. Metyrapone, 54-36-4; cytochrome P-450, 9035-51-2.

Supplementary Material Available: Lists of calculated and observed structure factor amplitudes (9 pages). Ordering information is given on any current masthead page.

(27) Bernstein, H. J.; Andrews, L. C.; Berman, H. M.; Bernstein, F. C.; Campbell, G. H.; Carrell, H. L.; Chaing, H. B.; Hamilton, W. C.; Jones, D. D.; Klunk, D.; Koetzle, T. F.; Meyer, E. F.; Morimoto, C. N.; Sevian, S. S.; Stodola, R. K.; Strongson, M. M.; Silloughby, T. V. "CRYSNET. A Network of Intelligent Remote Graphics Terminals"; Brookhaven National Laboratory: Upton, NY; report BNL 18803, p 148.
(28) Gantzel, P. K.; Sparks, R. A.; Long, R. E.; Trueblood, K. N. UCLALS4, 1969; program in Fortran IV.
(29) Carrell, H. L. "ICRFMLS. Modification of UCLALS4"; Institute for Cancer Research: Philadelphia, 1975; program from the Institute for Cancer Research.
(30) Carrell, H. L.; Shieh, H. S.; Takusagawa, F.; Wood, W. P., "Crystallographic Programs from the Institute for Cancer Research"; Institute for Cancer Research: Philadelphia, 1978.
(31) Cromer, D. T.; Waber, J. T. *Acta Crystallogr.* **1965**, *18*, 104.
(32) Stewart, R. F.; Davidson, E. R.; Simpson, W. T. *J. Chem. Phys.* **1965**, *42*, 3175.

Structural Requirements of Olefinic 5-Substituted Deoxyuridines for Antiherpes Activity†

John Goodchild,*‡ Roderick A. Porter,‡ Robert H. Raper,§ Iain S. Sim,§ Roger M. Upton,‡ Julie Viney,‡ and Harry J. Wadsworth‡

Departments of Chemistry and Biology, Searle Research and Development, Division of G.D. Searle and Co. Ltd., High Wycombe, Buckinghamshire, United Kingdom. *Received January 31, 1983*

A number of structurally related 5-substituted pyrimidine 2′-deoxyribonucleosides were synthesized and tested for antiviral activity against herpes simplex virus type 1 (HSV-1) in cell culture. A minimum inhibitory concentration was determined for each compound, and from a comparison of these values a number of conclusions were drawn with regard to those molecular features that enhance or reduce antiviral activity. Optimum inhibition of HSV-1 in cell culture occurred when the 5-substituent was unsaturated and conjugated with the pyrimidine ring, was not longer than four carbon atoms in length, had *E* stereochemistry, and included a hydrophobic, electronegative function but did not contain a branching point. Such features are contained in (*E*)-5-(2-bromovinyl)-2′-deoxyuridine, which was the most active of the compounds described.

Attempts to identify chemical antiviral agents that allow the effective and safe control of virus diseases of man have been largely unsuccessful. However, a number of nucleoside analogues are known that inhibit herpes simplex virus (HSV) replication.[1,2] The extent to which these inhibit virus growth without causing cellular toxicity reflects their degree of selectivity in reacting with virus-specific functions rather than interfering with cellular metabolism. There is evidence that the mechanism of action of these nucleoside analogues involves virus-coded enzymes important in DNA replication, and the exploitation of differences between virus-specific enzymes and the corresponding host cell enzymes provides a promising strategy in the search for more effective and less toxic antiherpes drugs.

The mechanism of action of the known antiviral nucleosides is, in many cases, not clearly defined. It has been proposed that some may interact with the virus-coded DNA polymerase[3-5] either as substrates or inhibitors, while others inhibit thymidylate synthetase.[6] However, such

† This work was first presented at the North American Medicinal Chemistry Symposium, June 1982.
‡ Department of Chemistry.
§ Department of Biology.

(1) De Clercq, E.; Torrence, P. F. *J. Carbohydr., Nucleosides, Nucleotides* **1978**, *5*, 187-224.
(2) De Clercq, E. *Acta Microbiol. Acad. Sci. Hung.* **1981**, *28*, 289-306.
(3) Furman, P. A.; St Clair, M. H.; Fyfe, J. A.; Rideout, J. L.; Keller, P. M.; Elion, G. B. *J. Virol.* **1979**, *32*, 72-77.
(4) Allaudeen, H. S.; Kozarich, J. W.; Bertino, J. R.; De Clercq, E. *Proc. Natl. Acad. Sci. U.S.A.* **1981**, *78*, 2698-2702.
(5) Ruth, J. L.; Cheng, Y.-C. *J. Biol. Chem.* **1982**, *257*, 10261-10266.
(6) De Clercq, E. *Methods Find. Exp. Clin. Pharmacol.* **1980**, *2*, 253-267.

0022-2623/83/1826-1252$01.50/0